Surface-Relief Gratings and Stable Birefringence Inscribed Using Light of Broad Spectral Range in Supramolecular Polymer-Bisazobenzene Complexes

Jenni E. Koskela,[†] Jaana Vapaavuori,[†] Juho Hautala,[†] Arri Priimagi,*,[†,§] Charl F. J. Faul,[‡] Matti Kaivola,[†] and Robin H. A. Ras*,[†]

[†]Department of Applied Physics and Center for New Materials, Aalto University, P.O. Box 15100, FI-00076 Aalto, Espoo, Finland
[‡]School of Chemistry, University of Bristol, Bristol BS8 1TS, United Kingdom
[§]Chemical Resources Laboratory, Tokyo Institute of Technology, R1-12, 4259 Nagatsuta, Midori-ku, Yokohama 226-8503, Japan

ABSTRACT: We report on phenol—pyridine hydrogen-bonded supramolecular polymer—azobenzene complexes made from a newly designed polar bisazobenzene chromophore. Because of the substitution with a polar nitro group, the chromophore possesses an extremely broad absorption band, spanning from near-UV up to 650 nm. Moreover, the inclusion of two methoxy groups to the central benzene ring prevents excessive chromophore—chromophore intermolecular interactions and provides advantageous size-related properties. Together, these features of the prepared photoresponsive polymer materials enable efficient inscription of (i) photoinduced birefringence with outstanding stability at various chromophore concentrations and (ii) surface-relief grating formation over a wide range of writing wavelengths from 405 to 633 nm. The photoresponsive behavior is compared to that of Disperse Yellow 7-based supramolecular complexes.
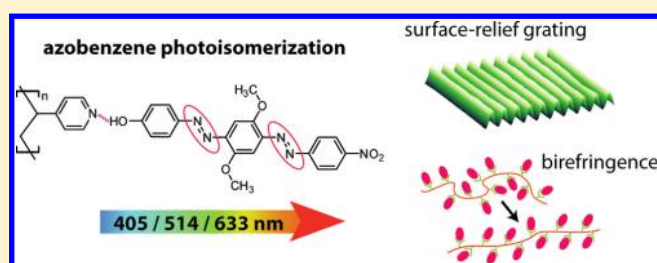
INTRODUCTION

The linear and nonlinear optical properties of azobenzene-containing polymers are of immense, yet unredeemed, technological interest. The potential applications are manifold, including, e.g., optical information storage and processing,[1,2] photoswitching,[3] diffractive optics,[4] and photomechanics.[5] Many of the attractive features are brought about by the photoisomerization of the azobenzene moieties, which not only act as an efficient photoswitch but also give rise to various large-scale molecular motions in the material system.[5−7] Perhaps the most widely studied phenomena are the photo-orientation of the azobenzene chromophores with polarized light and the photoinduced surface structuring upon irradiation with a light interference pattern, and many excellent reviews on the underlying photoinduced effects as well as their potential applications exist in literature.[3,5−11]

The photo-orientation efficiency of the material system depends delicately on factors such as the structure of the azobenzene moiety, type of bonding to the polymer as well as intermolecular interactions, and cooperative motions of the azobenzene moieties.[7] Photoinduced anisotropy has generally been observed to be higher and more stable in liquid-crystalline (LC) than in amorphous polymer systems due to strong cooperative movement and intermolecular interactions of the photochromic units.[12−14] The underlying mechanism for surface-relief grating (SRG) formation remains controversial to date, and none of the theoretical models[15−20] proposed to account for the driving force for this optical patterning technique

copes with all experimental observations. Yet the process depends strongly on, e.g., the molecular weight and the glass-transition temperature (T_g) of the host polymer[15,21,22] and the concentration[21,22] and polarity[15] of the azobenzene units. Efficient surface patterning also requires sufficiently strong bonding between the chromophores and the polymer backbone.[23,24] As opposed to being favorable for photo-orientation, strong intermolecular interactions and liquid crystallinity can significantly hinder the photoinduced mass transport required for SRG formation,[25,26] although many LC azo-polymer systems have also been reported to undergo efficient surface mass transport.[27−30] In order to fully exploit the potential of the light-induced phenomena of azobenzene-containing polymers, it is important to gain understanding on the structure—property relationships that govern their optical performance.

Supramolecular concepts provide excellent pathways toward attaining more comprehensive understanding on the role of chromophore concentration and chemical structure on the photoresponsive properties of the material system. Via supramolecular assembly, accomplished by noncovalent interactions between the polymer host and the chromophores, new functional materials can be created simply by mixing of readily available components, thus contrasting with the typical

time-consuming or costly organic synthesis of covalent polymer—dye systems.[31−33] Tuning of the chromophore concentration is effortless when compared to polymers with covalently bonded dyes, and even equimolar complexes, in which every polymer repeat unit is occupied by a dye molecule, can be fabricated without excessive aggregation or phase separation.[30,34] In addition, the noncooperative nature of hydrogen bonding allows facile control over the complexation degree as chromophores bind randomly to the polymer backbone.[31] A number of supramolecular polymer—azobenzene complexes with efficient photoresponsive properties have been demonstrated in recent years.[35−39] Noncovalent functionalization also provides the possibility to selectively remove the chromophores from the material system[24] and allows precise control over the molecular weight of the (separately synthesized) host polymer. These features render supramolecular functionalization strategies useful for both fundamental and application-oriented studies.

Bisazo-containing polymers have been reported to yield higher and more stable photoinduced birefringence than the corresponding monoazo-functionalized polymers owing to their large length-to-width ratio and low side-chain mobility.[40] The increased conjugation length and aspect ratio render bisazo-containing polymers promising for nonlinear optical applications[41] and have enabled designing bisazo-based polymeric materials with extremely high birefringence.[42,43] In a recent study by Wang and co-workers,[44] it was shown that the substitution pattern of the bisazo chromophore and the excitation wavelength greatly affect the photoinduced birefringence and SRG formation in epoxy-based bisazobenzene polymers. The study revealed, for example, that the SRG growth rate is significally improved when the middle benzene ring is 3,5-substituted with methyl groups, which they attribute to increased isomerization efficiency due to increased mutual distance between neighboring bisazo moieties. In another recent study, Wu et al.[39] showed that the magnitude and temporal stability of the photoinduced birefringence of a covalently functionalized azo-polymer were enhanced by hydrogen bonding between guest azobenzene units and azo groups of the host polymer, thus forming a supramolecular bisazo-polymer. With their materials design, they demonstrated an optical storage density of 0.93 Gbit/cm^2, which exceeds the storage density of a conventional DVD by a factor of 20.[39] In the course of our studies, we recently reported that complexes composed of a nonpolar bisazobenzene Disperse Yellow 7 (DY7) hydrogen-bonded to a poly(4-vinylpyridine) (P4VP) backbone yield highly efficient SRG formation with surface modulation depths as large as 600 nm.[45] The efficient SRG formation was attributed to the amorphous nature of these supramolecular spacer-free complexes; conversely, covalently functionalized bisazo-containing side-chain polymers have been reported to exhibit liquid crystallinity even when short spacers and moderate azobenzene concentrations are used.[46] Altogether, these former studies highlight the vast potential of bisazo-polymers for both photo-orientation and photoinduced surface-relief grating inscription.

To further clarify the role of chromophore polarity on the photoresponsive properties of hydrogen-bonded polymer—bisazobenzene complexes, we synthesized a polar bisazobenzene dye (abbreviated here as 2NHA), which exhibits attractive photoresponsive properties due to its molecular structure and broad absorption band. In this article, we describe the photo-orientation properties and SRG inscription in the 2NHA-based complexes and compare them to the previously studied

DY7-based complexes.[45] By tuning the molecular architecture, larger and substantially more stable photoinduced birefringence was obtained, while the range of efficient writing wavelengths was expanded significantly. Furthermore, SRG inscription was equally efficient as in the DY7-complexes and not obstructed by the large size of 2NHA.

■ EXPERIMENTAL SECTION

Synthesis of ((2,5-Dimethoxy-4-((4-nitrophenyl)diazenyl)-phenyl)diazenyl)phenol (2NHA). All reagents were purchased from Sigma-Aldrich and were used as received, unless otherwise stated. The Fast Black K salt provided was found to only contain ca. 40% diazonium salts and ca. 60% salt stabilizers. A typical synthetic methodology is provided, with quantities corrected for the stabilizer content. Ultrapure H$_2$O ($R > 18$ MΩ) was used throughout: Fast Black K hemi (zinc chloride) salt (2,5-dimethoxy-4-(4-nitrophenylazo)benzenediazonium chloride zinc double salt, 1.6 g, 3.83 mmol) was dissolved in H$_2$O (10 mL) and cooled to below 5 °C in an ice bath. Once cooled, the solution was added dropwise to a cold solution (<5 °C) of phenol (0.36 g, 3.83 mmol) and NaOH (0.153 g, 3.83 mmol) in H$_2$O (10 mL) over a 4 h period. The solution, left to stir overnight, was allowed to reach room temperature slowly. The obtained product was filtered and thoroughly washed with H$_2$O (5 × 50 mL). The solid was dried in vacuo and further purified by Soxhlet extraction with acetone as solvent and recrystallization from ethanol. The yield of the product was 0.99 g (63.5%). ^{1}H NMR (400 MHz, DMSO-$d6$, δ): 3.96 (s, 3H, CH3), 4.00 (s, 3H, CH3), 6.97 (d, J = 8.9 Hz, 2H, Ar H), 7.36 (s, 1H, Ar H), 7.45 (s, 1H, Ar H), 7.83 (d, J = 8.9 Hz, 2H, Ar H), 8.07 (d, J = 8.9 Hz, 2H, Ar H), 8.44 (d, J = 8.9 Hz, 2H, Ar H), 10.47 (br s, 1H, OH).

Complex Formation, Thin Film Preparation, and Characterization. 2NHA, poly(4-vinylpyridine) (P4VP, Polymer Source, Inc., M_n = 5100 g/mol, M_w = 5400 g/mol) and Disperse Yellow 7 (DY7, Sigma-Aldrich, 95%) were dissolved separately in tetrahydrofuran (THF, Sigma-Aldrich, >98%). After being stirred for at least 24 h, the solutions were filtered through 0.2 μm syringe filters, and the polymer—dye complexes were prepared by mixing the stock solutions in desired proportions. The prepared mixtures were stirred again for at least 24 h and then spin-coated on glass substrates. The film thickness was varied between 150 and 550 nm, as measured with a DEKTAK 6 M surface profiler. All sample films were of optically high quality with no sign of macroscopic phase separation or liquid-crystalline textures, as verified by polarized light microscopy (Leica DM4500P). The UV—vis absorption spectra of the films and of dilute chromophore solutions in THF were measured with a PerkinElmer Lambda 950 spectrometer. For infrared spectroscopy, solutions of the P4VP(2NHA)$_x$ complexes and pure 2NHA and P4VP were dropcast on silicon wafers, and the resulting samples were dried in vacuum overnight. The spectra were collected using a Nicolet 380 FTIR spectrometer by averaging 64 scans with resolution of 2 cm^{-1}. The FTIR measurement of the P4VP(DY7)$_y$ complexes has been previously described in ref 45.

Inscription of Birefringence and SRGs. The photo-orientation experiments were performed with the setup illustrated in Figure 1a, using excitation wavelengths of 405 nm (diode-pumped solid-state laser), 514 nm (Ar$^+$-laser), and 633 nm (He-Ne laser). The excitation was carried out using a vertically polarized beam with 100 mW/cm^2 intensity. The birefringence was monitored with a low-power probe beam (λ = 820 nm), whose transmission through
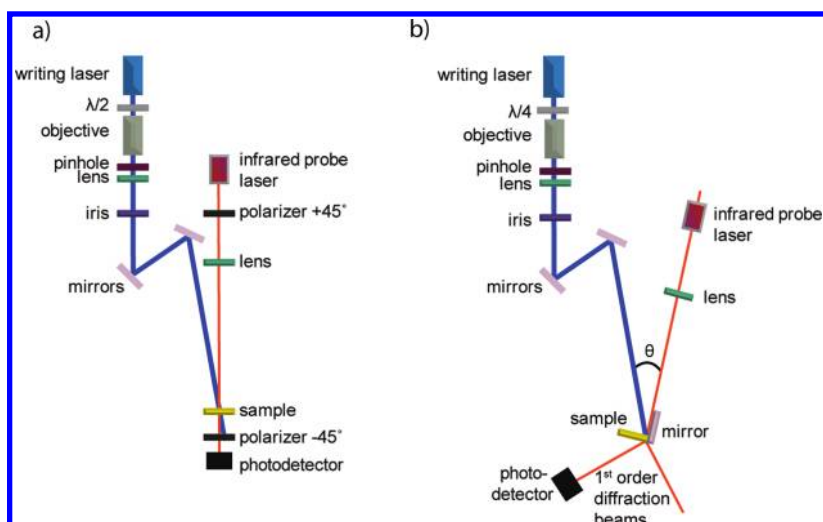
Figure 1. Schematic of the optical set-ups for inscription of (a) birefringence and (b) surface-relief gratings, both at writing wavelengths of 405, 514, and 633 nm.
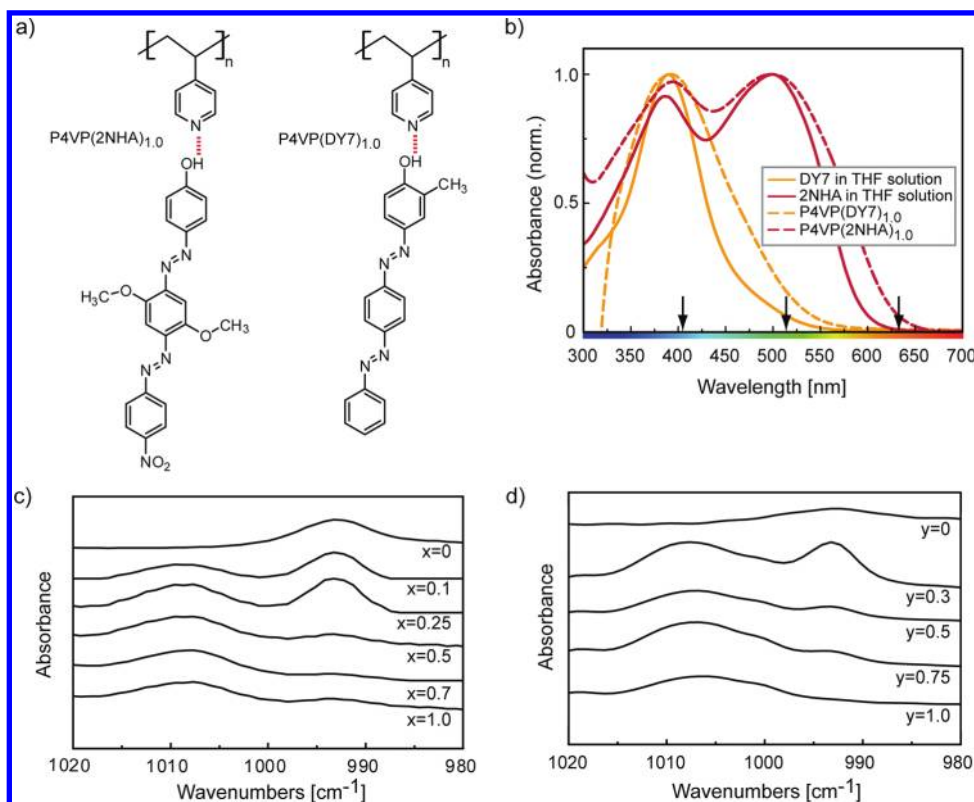
Figure 2. (a) Chemical structures of the nominally stoichiometric P4VP(2NHA)$_{1.0}$ and P4VP(DY7)$_{1.0}$ complexes, and (b) the normalized absorption spectra of thin films of P4VP(2NHA)$_{1.0}$ and P4VP(DY7)$_{1.0}$ and the solution spectra of 2NHA and DY7 in THF. The arrows point at the excitation wavelengths used in this study. The infrared spectra of (c) P4VP(2NHA)$_x$ and (d) P4VP(DY7)$_y$[45] complexes in which a shift of the pyridyl stretching peak from 993 cm^{-1} (pure polymer) to 1008 cm^{-1} is observed with increasing degree of complexation.

a polarizer/sample/analyzer configuration was measured in real time. The transmission direction of the polarizer/analyzer was set to $\pm 45°$ with respect to the polarization direction of the writing beam. The birefringence (Δn) values were calculated from

$$I = I_0 \sin^2\left(\frac{\pi |\Delta n| d}{\lambda}\right)$$

where d is the film thickness, λ the wavelength of the probe beam, I the intensity of the probe beam transmitted through the birefringent sample (polarizer and analyzer perpendicular), and I_0 the intensity through an unwritten sample (polarizer and analyzer parallel). Error estimation for the saturated birefringence values was done using the total differential of the birefringence equation ($\Delta I_0 = \pm 0.001$ V, $\Delta I = \pm 0.001$ V, $\Delta\lambda = \pm 1$ nm, and $\Delta d = \pm 10$ nm).

2365

dx.doi.org/10.1021/jp210706n |*J. Phys. Chem. C* 2012, 116, 2363–2370

Photoinduced SRGs were inscribed onto the sample films using circularly polarized (or s-polarized) light of 405, 514, or 633 nm with an intensity of 440, 300, or 150 mW/cm^2, respectively, in a Lloyd interferometer, as illustrated in Figure 1b. The interference pattern was generated by directing half of the incident beam directly onto the sample and by reflecting the other half from a mirror set at right angle with the sample. In this geometry, the grating period can be conveniently tuned by adjusting the angle between the incident beam and the sample plane. We set the period to approximately 1 μm. The inscription time was fixed to 45 min unless otherwise stated. The height profiles of the inscribed SRGs were determined by atomic force microscopy (Veeco Dimension 5000 SPM) a few days after the inscription process.

■ RESULTS AND DISCUSSION

From here on, the complexes are referred to as P4VP(2NHA)$_x$ and P4VP(DY7)$_y$, where x and y denote the degree of complexation (the number of chromophores per polymer repeat unit). The chemical structures of the complexes are shown in Figure 2a. As in our previous work,[26,37,45] phenol—pyridine hydrogen bonding is used to complex the dyes to the polymer backbone, as it enables easy tuning of the chromophore concentration even up to an equimolar degree of complexation. Also, 2NHA bears a phenolic moiety that can hydrogen bond with the pyridine group of P4VP. Upon hydrogen bond formation, the absorption band of the stretching mode of the free pyridine moieties shifts from 993 cm^{-1} to 1008 cm^{-1}.[47] The same shift is observed for P4VP(2NHA)$_x$ complexes, thus confirming hydrogen bond formation (Figure 2c). With an increasing degree of complexation, the relative intensity of the absorption band of the free pyridine moieties decreases gradually, until it almost completely vanishes at x = 0.70. For the equimolar P4VP(2NHA)$_{1.0}$ complex, the 993 cm^{-1} band does not vanish completely, which may indicate that full complexation is somewhat hindered by the lack of free space between the relatively bulky chromophores. As described previously in ref 45, the FTIR spectra of P4VP(DY7)$_y$ complexes (Figure 2d) shows the most pronounced peak shift for the y = 1.0 complex, suggesting complete complexation between the constituents.

The UV—vis absorption spectra for P4VP(2NHA)$_{1.0}$ and P4VP(DY7)$_{1.0}$ thin films and uncomplexed dyes in dilute THF solution are presented in Figure 2b. The aggregation induced blue-shift of the absorption band, while significant in, e.g., Disperse Red 1-based complexes,[34] are not present in the spectrum of complexed 2NHA or DY7. The slight broadening of the absorption peaks in the equimolar complexes compared to the peaks of the uncomplexed dyes can be attributed to chromophore—chromophore intermolecular interactions.[48] For both pure and complexed DY7, the absorption maximum is at around 390 nm, whereas for 2NHA, two almost equally intense absorption maxima can be observed at around 375 and 510 nm, attributed to the donor—acceptor structure containing the donating methoxy groups in the central phenyl ring and the electron withdrawing NO$_2$ moiety in the para position of the terminal phenyl group.

The photo-orientation efficiencies of P4VP(2NHA)$_x$ and P4VP(DY7)$_y$ complexes were determined from measurements of the photoinduced birefringence, as exemplified in Figure 3 for P4VP(2NHA)$_{0.7}$, the complex that exhibited the highest birefringence. The sample film is first illuminated with vertically polarized light until the saturation level of the birefringence is reached. The illumination is then ceased and the relaxation,
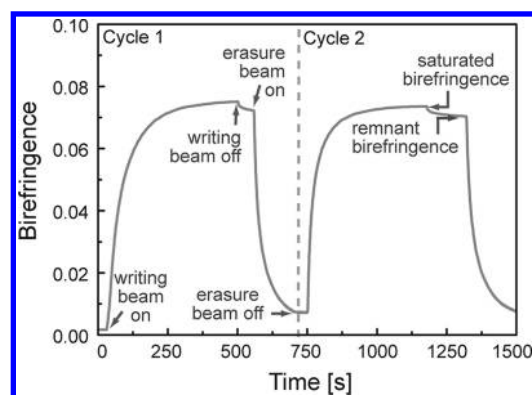
Figure 3. Typical curve for photoinduced birefringence as a function of writing time, in this case for the P4VP(2NHA)$_{0.7}$ complex, inscribed at 405 nm for two consecutive writing cycles.
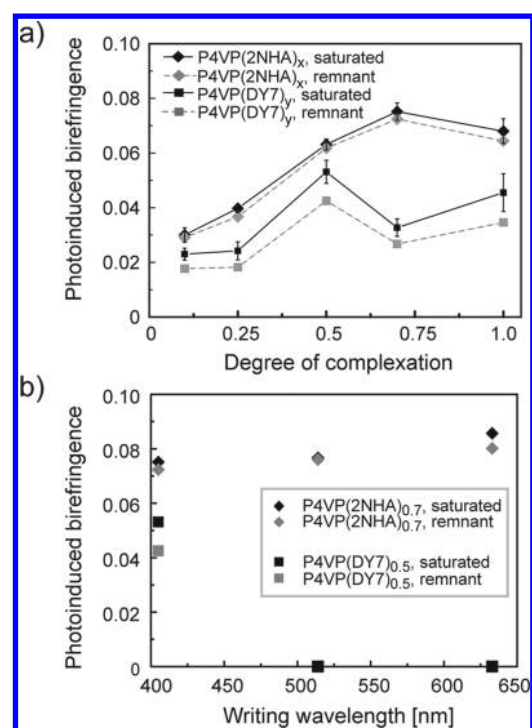
Figure 4. (a) Saturated and remnant photoinduced birefringence as a function of the degree of complexation at the writing wavelength of 405 nm. The P4VP(2NHA)$_x$ complexes produced higher and more stable birefringence than the corresponding P4VP(DY7)$_y$ complexes. The main source of error for the saturated birefringence values is film thickness, thus the slightly different thicknesses of the measured films directly correlate to the magnitude of the error bars. (b) Photoinduced birefringence as a function of the writing wavelength for P4VP-(2NHA)$_{0.7}$ and P4VP(DY7)$_{0.5}$, which produced the largest birefringence inscribed with the 405 nm beam. P4VP(2NHA)$_{0.7}$ exhibited equally efficient photo-orientation throughout the wide wavelength range used, unlike the P4VP(DY7)$_{0.5}$ complex.

which occurs due to thermal randomization of the chromophore orientation, is monitored until the decrease in the birefringence levels off and the remnant birefringence value can be determined. The extent of the relaxation depends, e.g., on the size of the chromophores and the T_g of the polymer,[14,40,49] but most importantly on the type of the dye—polymer interaction: covalently or noncovalently

2366

dx.doi.org/10.1021/jp210706n |*J. Phys. Chem. C* 2012, 116, 2363–2370

bonded chromophores are typically less mobile than chromophores in a guest—host system and thus have a much higher long-term stability of photo-orientation.[49,50] The remnant birefringence can be subsequently erased with a circularly polarized writing beam that randomizes the chromophore orientation in the plane of the sample film. The writing/relaxation/erasure cycle can be subsequently repeated, as illustrated in Figure 3.

Photoinduced birefringence was inscribed into the sample films using writing wavelengths of 405, 514, and 633 nm. The first two were selected based on the two absorption maxima of P4VP(2NHA)$_x$, whereas 633 nm was chosen to study the photoresponsivity of the material at a longer wavelength (see Figure 2b), far from the absorption maxima. For probing the photoinduced birefringence, a low power infrared laser (λ = 820 nm) was used in order to eliminate the possibility of photoisomerization/photo-orientation induced by the probe beam; as the low-energy absorption band of the 2NHA-based complexes extend well beyond 600 nm, even a low-power He—Ne probe beam (633 nm) quickly erased the birefringence after blocking the writing beam.

Figure 4a shows the saturated and remnant birefringence as a function of the degree of complexation at the writing wavelength of 405 nm for both P4VP(2NHA)$_x$ and P4VP(DY7)$_y$. The saturated birefringence of the P4VP(2NHA)$_x$ complexes increased systematically with dye concentration, being highest for x = 0.7. For P4VP(2NHA)$_{1.0}$, the photoinduced birefringence is slightly decreased, which is assumedly caused by less efficient complexation, as observed in the infrared spectrum, and less efficient trans—cis—trans isomerization cycling of the chromophores. Steric hindrance between the large dye molecules may lead to unfavorable chromophore—chromophore interactions, which in turn can reduce the optical performance of the material.[44] As seen in Figure 4a, relaxation of the birefringence is almost negligible in all P4VP(2NHA)$_x$ complexes. In contrast, both the magnitude and stability of photoinduced birefringence were significantly lower in P4VP(DY7)$_y$ than in the corresponding P4VP(2NHA)$_x$ complexes. No correlation between the chromophore concentration and the stability of the birefringence was observed in either of the materials, which is different from our previous studies on polymer-monoazobenzene systems where stabilization only takes place at high degrees of complexation.[26,37] It should also be noted that, according to the FTIR spectra, there is a difference between the real maximum degree of complexation between the two bisazobenzene materials, which makes it challenging to quantitatively compare the birefringence values of the corresponding 2NHA and DY7 complexes.

Photoinduced birefringence was also measured using the writing wavelengths of 514 and 633 nm for the complexes that showed the highest birefringence at 405 nm, i.e., P4VP(2NHA)$_{0.7}$ and P4VP(DY7)$_{0.5}$. Figure 4b presents the birefringence values for the three inscription wavelengths. For P4VP(2NHA)$_{0.7}$, the saturated birefringence values were nearly independent of the writing wavelength, and the temporal relaxation was negligible. The extremely wide absorption bands of 2NHA allow triggering the trans—cis—trans isomerization cycling, and subsequent photo-orientation, over a wide range of inscription wavelengths. Furthermore, according to the results of Wang et al. the methoxy spacers attached to the middle benzene ring are likely to play an important role in the photo-orientation; they not only broaden the absorption spectrum of the chromophore but they are also essential in preventing excessive dipolar interactions between the polar 2NHA molecules.[44] On the contrary,

we found that P4VP(DY7)$_{0.5}$ cannot be effectively photo-oriented at the longer wavelengths as no photoinduced birefringence was observed at the writing wavelengths of 514 or 633 nm. This behavior was somewhat expected, based on the absorption spectra of the pure and complexed DY7, but however, 514 nm lies well within the absorption tail of the chromophore, similarly as 633 nm lies in the absorption tail of 2NHA. We think that the fact that no birefringence could be induced in P4VP(DY7)$_{0.5}$ even at 514 nm is related to the nonpolar nature of DY7, which dramatically decreases the thermal cis—trans isomerization rate[51] and consequently suppresses the trans—cis—trans isomerization cycling required for photo-orientation.

The kinetics of photo-orientation was analyzed using the following biexponential model:[52]

$$\Delta n = A\left(1 - \exp\left(-\frac{t}{\tau_a}\right)\right) + B\left(1 - \exp\left(-\frac{t}{\tau_b}\right)\right)$$

where Δn is the birefringence at time t, and τ_a and τ_b are the time constants of the fast and slow growth components, respectively. The sum of coefficients A and B represents the value of the saturated birefringence, and individually they describe the contribution of the fast and slow component on the induced birefringence, respectively. The birefringence growth could be fitted well with the model, and the fitting parameters as well as the percentual contribution of the fast components are shown in Table 1 for P4VP(DY7)$_{0.5}$ and P4VP(2NHA)$_{0.7}$. During the experiments, very different saturation times were observed for 2NHA-based and DY7-based complexes; both the fast and the slow time constants are an order of magnitude smaller for P4VP(DY7)$_{0.5}$ than for P4VP(2NHA)$_{0.7}$. The quicker saturation of P4VP(DY7)$_{0.5}$ can be attributed to the domination of the fast growth component, which for this complex was almost 90%. We conclude that the induced birefringence in this complex arises mainly due to angular changes in the cis concentration and possibly local photo-orientation, not due to slower movements associated with the movement of the polymer segments or collaborative reorientation, which are typically seen in the slow growth component.[52] For P4VP(2NHA)$_{0.7}$, the contribution of the fast component was reduced to ca. 60%, indicating that the contribution of polymer chain movement to photo-orientation increases somewhat in importance.

The photo-orientation efficiency of P4VP(2NHA)$_x$ complexes increased significantly on the second writing cycle (see Figure 3). For P4VP(2NHA)$_{0.7}$, the time constants for the fast and slow growth components were 37 and 110 s for the first cycle and 11 and 63 s for the second cycle, respectively (Table 1). A possible reason for this could be the orientation of the polymer backbone during the first cycle. Even though the anisotropic chromophore alignment is randomized during illumination with circularly polarized light, the polymer backbone may stay aligned in a way that facilitates photo-orientation of the chromophores in the second cycle and thus makes it faster. This polymer chain alignment could also be a plausible explanation why the photoinduced birefringence is not completely reduced to zero after erasure in Figure 3.

Compared to the chemical structure of the nonpolar DY7, 2NHA has no methyl group ortho to the hydrogen-bonding hydroxyl group, but two additional methoxy groups are attached to the middle benzene ring and an electron-withdrawing nitro group attached to the terminal benzene ring in para position. The push—pull-type 2NHA thus exhibits a larger dipole moment,

Table 1. Time Constant Parameters for Birefringence Growth Using 405 nm Inscription Wavelength in P4VP(2NHA)0.7 and P4VP(DY7)0.5, Calculated As $A_n = A/(A + B)$, and the Percentual Contribution of the Fast Component A_n

parameter	P4VP(2NHA)$_{0.7}$ first cycle	P4VP(2NHA)$_{0.7}$ second cycle	P4VP(DY7)$_{0.5}$
A	0.05	0.04	0.05
τ_a (s)	37.07	11.08	1.27
B	0.03	0.03	0.01
τ_b (s)	110.28	63.12	6.50
A_n	0.61	0.57	0.88

Figure 5. (a) Typical AFM height profile of an SRG, inscribed on a thin film of P4VP(2NHA)$_{0.7}$ showing a uniform sinusoidal surface pattern. (b) Average modulation depths as a function of the complexation degree for SRGs inscribed on P4VP(2NHA)$_x$ sample films with writing wavelengths of 405, 514, and 633 nm.

which in turn enables stronger interaction between the chromophores, while in P4VP(DY7)$_y$ such interactions are much weaker. Intermolecular interactions decrease the mobility of the chromophores, thus making the photo-orientation more stable,[37,39] while excessive chromophore aggregation is prevented by the methoxy groups.[44] Maybe even more importantly, 2NHA is more bulky than DY7 due to the two methoxy groups. Bulky substituents near the photoisomerizable groups hinder chromophore motion, which on the one hand explains the long writing time required for P4VP(2NHA)$_x$ but on the other hand makes the relaxation process more difficult, thus giving rise to enhanced temporal stability.[53] The lower mobility due to bulkier 2NHA chromophores also explains the substantial difference in the saturation times with P4VP(DY7)$_y$, even if the push−pull nature of 2NHA should accelerate the writing process.[7] Wang et al.[44] proposed that the bulky substituents such as methyl groups on the bisazobenzenes can have two counteracting effects on photoisomerization: they can either promote it by reducing aggregation or they can act as a steric hindrance and inhibit it. In the present case, the methoxy groups in the middle ring seem to be beneficial in terms of efficient photoisomerization. To conclude, the intermolecular interactions and bulkiness arising from the molecular structure of the 2NHA molecules are thought to contribute to the excellent stability of photo-orientation in P4VP(2NHA)$_x$ observable as high remnant birefringence.

The mass-transport efficiency of P4VP(2NHA)$_x$ complexes was investigated by inscribing SRGs on the sample films at three different writing wavelengths with a circularly polarized beam. SRGs were successfully inscribed in films of all degrees of complexation, even though the gratings in the $x = 0.1$ complexes remained very shallow. We note that when the s-polarized beam was used for inscription, no SRGs were formed in the sample films as there is no polarization component in the direction of the grating vector. Hence, we can rule out any significant contribution of thermal effects or photodegradation on SRG formation in the present materials. A typical AFM image of an SRG is shown in Figure 5a. No significant differences in the modulation depths can be observed between the writing wavelengths 405 and 514 nm (Figure 5b). As expected, the average modulation depth increased as the complexation degree increased up to $x = 0.5$, after which the depth growth leveled off. In fact, the equimolar complexes ($x = 1.0$) produced somewhat shallower gratings, which is consistent with the facts that, (i) based on the FTIR spectra, complete complexation could not be obtained for these complexes and that (ii) the photoinduced birefringence was somewhat lower in the equimolar complex. Besides the possibility of less
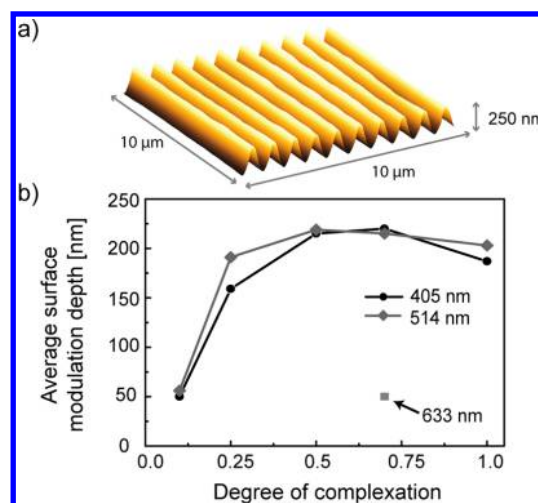
efficient complexation, this decay in the average modulation depth can be attributed to reduced mobility of the chromophores caused by lesser free volume within the material in combination with larger molecular weight, as has been observed also for P4VP(DY7)$_y$.[45] Altogether, the bulkiness of 2NHA compared to DY7 did not significantly reduce the mass-transport ability of the material, as the average modulation depths at $x = 0.5$ and $x = 0.7$ were close to the original thickness of the films (250 nm). Previously, it has been reported that rod-like and polar dye substituents in hydrogen-bonded monoazo complexes seem to suppress the mass transport by promoting the formation of mesophase,[26] but this is obviously not the case with 2NHA. Even if there are intermolecular interactions stabilizing the system, no LC structure could be observed in the studied films, and the material appears flexible and mobile enough for efficient SRG formation, presumably due to the methoxy groups attached to the central phenyl ring. Moreover, the formation of an LC phase is suppressed in both of the studied complexes as there is no flexible spacer between the chromophores and the polymer backbone.[13]

Similar concentration dependence in the SRG modulation depth as shown in Figure 5b has been reported also in covalently functionalized azo-polymers by Fukuda et al.[21] and Börger et al.[54] On the contrary, Andruzzi et al. have reported on dramatic suppression of the surface relief in side-chain polymethacrylates at azobenzene concentrations exceeding 75 mol %, probably due to existence of LC phases at high degree of functionalization,[28] and Priimagi et al. reported on the linear increase in the surface-modulation depth up to equimolar complexation in amorphous polymer−monoazo complexes.[22] The fact that the concentration dependence of SRG formation differs considerably for different azobenzene-containing materials serves to highlight the complicated nature of this photomechanical effect, which is not comprehensively understood up to date.

Lastly, besides using the conventional writing wavelengths of 405 and 514 nm, we were able to inscribe an SRG also using a 633 nm writing beam. The efficiency of the SRG formation was

2368

dx.doi.org/10.1021/jp210706n |J. Phys. Chem. C 2012, 116, 2363–2370

substantially reduced due to the low absorbance of the material at 633 nm. Within a 90 min writing time used, an SRG with an average modulation depth of approximately 50 nm was inscribed on the P4VP(2NHA)$_{0.7}$ sample (Figure 5b). Moreover, due to the power limitations of the writing laser, the intensity of the inscription beam was only half of the intensity used at the shorter wavelengths. We are confident that with improvements to the inscription setup, such as increased laser intensity and laser beam quality, one could effectively achieve SRGs with higher modulation depths for the red writing beam.

Last year, Ozols et al.[55,56] reported on SRGs in azobenzene-containing molecular glass recorded with a 633 nm beam. In their work, azobenzene photodegradation caused by the red beam is thought to contribute to SRG formation. This is most likely not the case in our study, as efficient photo-orientation of the chromophores was achieved for the 633 nm writing beam. Moreover, the fact that no SRGs could be inscribed with an *s*-polarized beam supports the idea of photoisomerization-induced surface patterning. We also note that very recently, Goldenberg and co-workers published an efficient SRG formation at 633 nm in a low-molecular weight azobenzene-containing material.[57] The absorption maximum of their system was at 495 nm, and they successfully used inscription wavelengths of 488 nm, 532 nm, and 633 nm. In our case, we anticipate the range of possible inscription wavelengths to be even broader due to the very broad double-peak electronic absorption spectrum; the true limits are yet to be tested even if wavelength span exceeding 200 nm has been demonstrated here. Hence, by using supramolecular assembly and smart chromophore design, it is possible to produce materials with enhanced and easily tailorable photoresponsive properties.

CONCLUSIONS

Using the newly synthesized 2NHA dye, supramolecular polymer-bisazobenzene complexes with versatile photoresponsive properties were prepared. They enabled photoinduced birefringence with excellent photoalignment stability and surface-relief gratings throughout a wide concentration range and wide range of possible inscription wavelengths, even beyond 600 nm. We foresee that the combination of the flexible supramolecular concept with the possibility to use a very broad range of the visible spectrum for both photo-orientation and macroscopic mass-transport will enable new applications for photoresponsive materials.

AUTHOR INFORMATION

Corresponding Author
*E-mail: arri.priimagi@aalto.fi (A.P.); robin.ras@aalto.fi (R.H.A.R.).

ACKNOWLEDGMENT

ABBREVIATIONS

SRG, surface-relief grating; P4VP, poly(4-vinyl pyridine); DY7, Disperse Yellow 7; 2NHA, ((2,5-dimethoxy-4-((4-nitrophenyl)diazenyl)-phenyl)diazenyl)phenol; AFM, atomic force microscopy

REFERENCES

(1) Hvilsted, S.; Sanchez, C.; Alcala, R. *J. Mater. Chem.* **2009**, *19*, 6641–6648.

(2) Huang, W. H.; Hu, Y. L.; Zhang, Z. S.; Chen, Y. H.; Zhang, Q. *J. Opt. Lett.* **2010**, *35*, 46–48.

(3) Yager, K. G.; Barrett, C. J. *J. Photochem. Photobiol., A* **2006**, *182*, 250–261.

(4) Alasaarela, T.; Zheng, D.; Huang, L.; Priimagi, A.; Bai, B.; Tervonen, A.; Honkanen, S.; Kuittinen, M.; Turunen, J. *Opt. Lett.* **2011**, *36*, 2411–2413.

(5) Barrett, C. J.; Mamiya, J.-I.; Yager, K. G.; Ikeda, T. *Soft Matter* **2007**, *3*, 1249–1261.

(6) Viswanathan, N. K.; Kim, D. Y.; Bian, S. P.; Williams, J.; Liu, W.; Li, L.; Samuelson, L.; Kumar, J.; Tripathy, S. K. *J. Mater. Chem.* **1999**, *9*, 1941–1955.

(7) Natansohn, A.; Rochon, P. *Chem. Rev.* **2002**, *102*, 4139–4175.

(8) Delaire, J. A.; Nakatani, K. *Chem. Rev.* **2000**, *100*, 1817–1845.

(9) Yesodha, S. K.; Pillai, C. K. S.; Tsutsumi, N. *Prog. Polym. Sci.* **2004**, *29*, 45–74.

(10) Shishido, A. *Polym. J.* **2010**, *42*, 525–533.

(11) Beharry, A. A.; Woolley, G. A. *Chem. Soc. Rev.* **2011**, *40*, 4422–4437.

(12) Stumpe, J.; Läsker, L.; Fischer, T.; Rutloh, M.; Kostromin, S.; Ruhmann, R. *Thin Solid Films* **1996**, *284–285*, 252–256.

(13) Han, M.; Morino, S. Y.; Ichimura, K. *Macromolecules* **2000**, *33*, 6360–6371.

(14) Freiberg, S.; Lagugné-Labarthet, F. O.; Rochon, P.; Natansohn, A. *Macromolecules* **2003**, *36*, 2680–2688.

(15) Barrett, C. J.; Natansohn, A. L.; Rochon, P. L. *J. Phys. Chem.* **1996**, *100*, 8836–8842.

(16) Pedersen, T. G.; Johansen, P. M.; Holme, N. C. R.; Ramanujam, P. S.; Hvilsted, S. *Phys. Rev. Lett.* **1998**, *80*, 89–92.

(17) Kumar, J.; Li, L.; Jiang, X. L.; Kim, D. Y.; Lee, T. S.; Tripathy, S. *Appl. Phys. Lett.* **1998**, *72*, 2096–2098.

(18) Lefin, P.; Fiorini, C.; Nunzi, J. M. *Pure Appl. Opt.* **1998**, *7*, 71–82.

(19) Saphiannikova, M.; Neher, D. *J. Phys. Chem. B* **2005**, *109*, 19428–19436.

(20) Plain, J.; Juan, M. L.; Bachelot, R.; Royer, P.; Gray, S. K.; Wiederrecht, G. P. *ACS Nano* **2009**, *3*, 1573–1579.

(21) Fukuda, T.; Matsuda, H.; Shiraga, T.; Kimura, T.; Kato, M.; Viswanathan, N. K.; Kumar, J.; Tripathy, S. K. *Macromolecules* **2000**, *33*, 4220–4225.

(22) Priimagi, A.; Lindfors, W.; Kaivola, M.; Rochon, P. *ACS Appl. Mater. Interfaces* **2009**, *1*, 1183–1189.

(23) Fiorini, C.; Prudhomme, N.; de Veyrac, G.; Maurin, I.; Raimond, P.; Nunzi, J. M. *Synth. Met.* **2000**, *115*, 121–125.

(24) Zettsu, N.; Ogasawara, T.; Mizoshita, N.; Nagano, S.; Seki, T. *Adv. Mater.* **2008**, *20*, 516–521.

(25) You, F. X.; Paik, M. Y.; Hackel, M.; Kador, L.; Kropp, D.; Schmidt, H. W.; Ober, C. K. *Adv. Funct. Mater.* **2006**, *16*, 1577–1581.

(26) Vapaavuori, J.; Valtavirta, V.; Alasaarela, T.; Mamiya, J.-I.; Priimagi, A.; Shishido, A.; Kaivola, M. *J. Mater. Chem.* **2011**, *21*, 15437–15441.

(27) Ubukata, T.; Seki, T.; Ichimura, K. *Adv. Mater.* **2000**, *12*, 1675–1678.

(28) Andruzzi, L.; Altomare, A.; Ciardelli, F.; Solaro, R.; Hvilsted, S.; Ramanujam, P. S. *Macromolecules* **1999**, *32*, 448–454.

(29) Seki, T.; Zettsu, N.; Ogasawara, T.; Arakawa, R.; Nagano, S.; Ubukata, T. *Macromolecules* **2007**, *40*, 4607–4613.

(30) Zhang, Q.; Wang, X.; Barrett, C. J.; Bazuin, C. G. *Chem. Mater.* **2009**, *21*, 3216–3227.

(31) Faul, C. F. J.; Antonietti, M. *Adv. Mater.* **2003**, *15*, 673–683.

(32) Ikkala, O.; ten Brinke, G. *Chem. Commun.* **2004**, 2131–2137.

(33) Pollino, J. M.; Weck, M. *Chem. Soc. Rev.* **2005**, *34*, 1078–1078.

(34) Priimagi, A.; Cattaneo, S.; Ras, R. H. A.; Valkama, S.; Ikkala, O.; Kauranen, M. *Chem. Mater.* **2005**, *17*, 5798–5802.

(35) Kulikovska, O.; Goldenberg, L. M.; Stumpe, J. *Chem. Mater.* **2007**, *19*, 3343–3348.

(36) Gao, J.; He, Y. N.; Xu, H. P.; Song, B.; Zhang, X.; Wang, Z. Q.; Wang, X. G. *Chem. Mater.* **2007**, *19*, 14–17.

(37) Priimagi, A.; Vapaavuori, J.; Rodriguez, F. J.; Faul, C. F. J.; Heino, M. T.; Ikkala, O.; Kauranen, M.; Kaivola, M. *Chem. Mater.* **2008**, *20*, 6358–6363.

(38) Mamiya, J. I.; Yoshitake, A.; Kondo, M.; Yu, Y.; Ikeda, T. *J. Mater. Chem.* **2008**, *18*, 63–65.

(39) Wu, S.; Duan, S. Y.; Lei, Z. Y.; Su, W.; Zhang, Z. S.; Wang, K. Y.; Zhang, Q. J. *J. Mater. Chem.* **2010**, *20*, 5202–5209.

(40) Meng, X.; Natansohn, A.; Rochon, P. *Polymer* **1997**, *38*, 2677–2682.

(41) Wang, X.; Kumar, J.; Tripathy, S. K.; Li, L.; Chen, J.-I.; Marturunkakul, S. *Macromolecules* **1997**, *30*, 219–225.

(42) Lachut, B. L.; Maier, S. A.; Atwater, H. A.; de Dood, M. J. A.; Polman, A.; Hagen, R.; Kostromine, S. *Adv. Mater.* **2004**, *16*, 1746–1750.

(43) Fukuda, T.; Kim, J. Y.; Barada, D.; Senzaki, T.; Yase, K. *J. Photochem. Photobiol., A* **2006**, *182*, 262–268.

(44) Wang, X.; Yin, J.; Wang, X. *Polymer* **2011**, *52*, 3344–3356.

(45) Vapaavuori, J.; Priimagi, A.; Kaivola, M. *J. Mater. Chem.* **2010**, *20*, 5260–5264.

(46) Cojocariu, C.; Rochon, P. *Macromolecules* **2005**, *38*, 9526–9538.

(47) Ruokolainen, J.; ten Brinke, G.; Ikkala, O.; Torkkeli, M.; Serimaa, R. *Macromolecules* **1996**, *29*, 3409–3415.

(48) Kelley, A. M. *J. Chem. Phys.* **2003**, *119*, 3320–3331.

(49) Natansohn, A.; Rochon, P.; Barrett, C.; Hay, A. *Chem. Mater.* **1995**, *7*, 1612–1615.

(50) Priimagi, A.; Kaivola, M.; Rodriguez, F. J.; Kauranen, M. *Appl. Phys. Lett.* **2007**, *90*, 121103.

(51) Barrett, C.; Natansohn, A.; Rochon, P. *Chem. Mater.* **1995**, *7*, 899–903.

(52) Ho, M. S.; Natansohn, A.; Rochon, P. *Macromolecules* **1995**, *28*, 6124–6127.

(53) Cojocariu, C.; Rochon, P. *Pure Appl. Chem.* **2004**, *76*, 1479–1497.

(54) Borger, V.; Kuliskovska, O.; Hubmann, K. G.; Stumpe, J.; Huber, M.; Menzel, H. *Macromol. Chem. Phys.* **2005**, *206*, 1488–1496.

(55) Ozols, A.; Kokars, V.; Augustovs, P.; Traskovskis, K.; Maleckis, A.; Mezinskis, G.; Pludons, A.; Saharov, D. *Opt. Mater.* **2010**, *32*, 811–817.

(56) Ozols, A.; et al. *J. Phys.: Conf. Ser.* **2010**, *249*, 012055.

(57) Goldenberg, L. M.; Gritsai, Y.; Stumpe, J. *J. Opt.* **2011**, *13*, 075601.